Electronic supplementary materials *Mendeleev Commun.*, 2024, **34**, 74–77

Ru^{II} and Ru^{III} complexes with 2,6-di-*tert*-butylphenol ligands: synthesis, electrochemical behaviour, antioxidant properties and antiproliferative activity

Anastasia A. Antonets, Ksenia M. Voroshilkina, Ilya A. Shutkov, Dmitrii M. Mazur, Vladimir Yu. Tyurin, Ludmila G. Dubova, Elena F. Shevtsova, Alexey A. Nazarov and Elena R. Milaeva

Materials and Methods

All solvents were purified and degassed before use.[S1] *N*-(3-(1*H*-Imidazol-1-yl)propyl)-3,5-di-*tert*-butyl-4-hydroxybenzamide (**1**) was prepared following the published procedure.[S2] NMR spectra were recorded on a Bruker Avance II 400 spectrometer at room temperature at 400.13 (^{1}H) MHz at the concentration 10-20 mM. Chemical shifts were referenced relative to the solvent signal for ^{1}H. Elemental analysis was performed with MicroCube Elementar analyzer. Electrospray ionization (ESI) mass spectra were recorded using a TSQ Endura (Thermo Fisher Scientific, Waltham, MA, USA) instrument. Each analysed compound was dissolved in methanol (HPLC grade) and injected directly into the ionization source through a syringe pump. The spectra were recorded during 30 s in the *m/z* range 150–1400 in both positive and negative ionization modes with spray voltage 3.4 and 2.5 kV, correspondingly at the concentrations varied within 100-1000 μg L^{-1} range.

3.1. Synthesis

N-(3-(1*H*-Imidazol-1-yl)propyl)-2-(3,5-di-*tert*-butyl-4-hydroxyphenyl)acetamide (**2**)

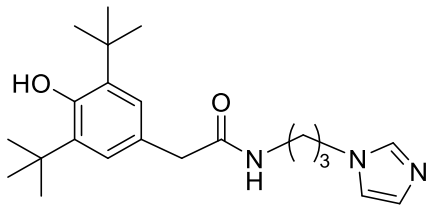

Oxalyl chloride (0.96 mL, 10.8 mmol) and a catalytic amount of DMF were added to a solution of 3,5-di-*tert*-butyl-4-hydroxyphenylacetic acid (300 mg, 1.08 mmol) in $CHCl_3$ (20 mL). The reaction mixture was stirred at 50°C for 3 h. The solvent and oxalyl chloride were removed in a vacuum. The obtained crude acid chloride was dissolved in DCM (dichloromethane, 20 mL), and 1-(3-aminopropyl)imidazole (334 μL, 2.84 mmol) was added with stirring. The reaction mixture was stirred at room temperature for 12 h. The solution was filtered and evaporated up to a minimum volume. The product was purified by column chromatography on silica gel (eluent: EtOAc : EtOH (8:1), R_f = 0.15). The colourless product was dried in a vacuum. Yield: 203 mg (48%), m.p. 118–122°C, elem. anal. calc. (%) for $C_{22}H_{33}N_3O_2 \times 0.5\ CH_3CH_2OH$: C 70.02, H 9.20, N 10.65. Found C 69.92, H 9.49, N 11.28. ESI MS m/z: 370 $[M - H]^-$, 372 $[M + H]^+$. ^{1}H NMR (400.13 MHz, $CDCl_3$, δ ppm): 7.37 (br.s, 1H, N-CH=N), 7.03 (br.s, 1H, N=CH-CH), 7.02 (s, 2H, C=CH-C), 6.84 (br.s, 1H, CH-CH=N), 5.56 (s, 1H, N-H), 5.26 (s, 1H, O-H), 3.91 (т, 2H, J = 6.9 Hz, CH_2-CH_2-N), 3.21 (q, 2H, J = 6.6 Hz, NH-CH_2-CH_2), 1.96 (п, 2H, J = 6.9 Hz, CH_2-CH_2-CH_2), 1.44 (s, 20H, C-CH_3, C_{Ar}-CH_2-CO).

Dichlorido(η^6-*p*-cymene){*N*-[3-(1*H*-imidazol-1-yl)propyl]-3,5-di-*tert*-butyl-4-hydroxybenzamide}ruthenium(II) (**3**)

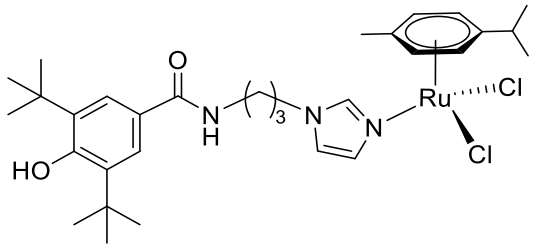

A solution of **1** (94 mg, 0.26 mmol) in dry DCM (5 mL) was added to a solution of bis[dichlorido(η^6-*p*-cymene)ruthenium(II)] (78 mg, 0.13 mmol) in dry DCM (15 mL). The reaction mixture was stirred at room temperature for 12 h. The solution was evaporated up to a minimum volume. The red-brown product was precipitated by the addition of ethyl acetate, filtered, washed with ether and dried in a vacuum. Yield: 123 mg (71%), m.p. 186–189°C, elem. anal. calc. (%) for $C_{31}H_{45}Cl_2N_3O_2Ru \times 0.4\ CH_2Cl_2$: C 54.06, H 6.62, N 6.02. Found: C 53.76, H 6.83, N 6.12. ESI MS m/z: 628 $[M - Cl]^+$. ^{1}H NMR (400.13 MHz, $CDCl_3$, δ ppm): 7.87 (br.s, 1H, N-C<u>H</u>=N), 7.66 (s, 2H, C=C<u>H</u>-C), 7.20 (br.s, 1H, N=C<u>H</u>-CH), 6.88 (br.s, 1H, CH=C<u>H</u>-N), 6.79 (t, 1H, J = 5.7 Hz, N-<u>H</u>), 5.56 (s, 1H, O-<u>H</u>), 5.41 (d, 2H, J = 5.9 Hz, C-C<u>H</u>=CH), 5.24 (d, 2H, J = 6.0 Hz, CH=C<u>H</u>-C), 3.77 (t, 2H, J = 7.3 Hz, CH_2-C<u>H_2</u>-N), 3.33 (q, 2H, J = 6.4 Hz, NH-C<u>H_2</u>-CH_2), 2.98-2.91 (m, 1H, CH_3-C<u>H</u>-CH_3), 2.16 (s, 3H, C_{Ar}-C<u>H_3</u>), 1.88-1.78 (m, 2H, CH_2-C<u>H_2</u>-CH_2), 1.48 (s, 18H, C-C<u>H_3</u>), 1.27 (d, 6H, J = 6.9 Hz, C<u>H_3</u>-CH-C<u>H_3</u>).

Dichlorido(η^6-*p*-cymene){*N*-[3-(1*H*-imidazol-1-yl)propyl]-2-(3,5-di-*tert*-butyl-4-hydroxyphenyl)acetamide}ruthenium(II) (**4**)

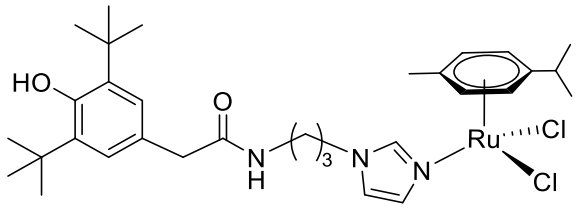

A solution of **2** (85 mg, 0.24 mmol) in dry DCM (4 mL) was added to a solution of bis[dichlorido(η^6-*p*-cymene)ruthenium(II)] (70 mg, 0.12 mmol) in dry DCM (14 mL). The reaction mixture was stirred at room temperature for 12 h. The solvent was removed, and the red-brown product was washed with ether and dried in a vacuum. Yield: 110 mg (72%), m.p. 123–126°C, elem. anal. calc. (%) for $C_{32}H_{47}Cl_2N_3O_2Ru \times 0.1\ CH_2Cl_2$: C 56.18, H 6.93, N 6.12. Found: C 56.01, H 7.07, N 6.23. ESI MS m/z: 642 $[M - Cl]^+$. ^{1}H NMR (400.13 MHz, $CDCl_3$, δ ppm): 7.89 (br.s, 1H, N-C<u>H</u>=N), 7.24 (br.s, 1H, N=C<u>H</u>-CH), 7.09 (s, 2H, C=C<u>H</u>-C), 6.83 (br.s, 1H, CH=C<u>H</u>-N), 6.26 (s, 1H, N-<u>H</u>), 5.45 (d, 2H, J = 6.0 Hz, C-C<u>H</u>=CH), 5.25 (d, 2H, J = 6.0 Hz, CH=C<u>H</u>-C), 5.16 (s, 1H, O-<u>H</u>), 3.73 (t, 2H, J = 7.2 Hz, CH_2-C<u>H_2</u>-N), 3.47 (s, 2H, C_{Ar}-C<u>H_2</u>-CO), 3.12-3.08 (м , 2H, NH-C<u>H_2</u>-CH_2), 2.98-2.91 (м, 1H, CH_3-C<u>H</u>-CH_3), 2.13 (s, 3H, C_{Ar}-C<u>H_3</u>), 1.75-1.64 (м, 2H, CH_2-C<u>H_2</u>-CH_2), 1.44 (s, 18H, C-C<u>H_3</u>), 1.28 (d, 6H, J = 6.9 Hz, C<u>H_3</u>-CH-C<u>H_3</u>).

Oxalato(η^6-*p*-cymene){*N*-[3-(1*H*-imidazol-1-yl)propyl]-3,5-di-*tert*-butyl-4-hydroxybenzamide}ruthenium(II) (**5**)

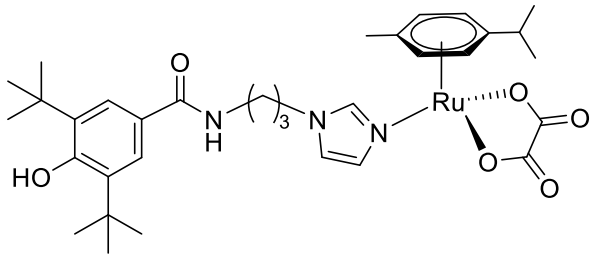

A suspension of silver oxalate (60 mg, 0.20 mmol) in water (5 ml) was added to a solution of bis[dichlorido(η^6-*p*-cymene)ruthenium(II)] (60 mg, 0.10 mmol) in water (23 ml). The reaction mixture was stirred at room temperature for 12 h. The solution was filtered and the solvent was removed. The solid product was dissolved in MeOH (13 ml) and added to a solution of **1** (70 mg, 0.20 mmol) in a minimum amount of MeOH. The reaction mixture was stirred at room temperature for 12 h. The product was purified by column chromatography on silica gel (eluent: EtOAc : MeOH (2:1), R_f = 0.50). The obtained yellow product was dried in a vacuum. Yield: 97 mg (73%), m.p. 178–183°C (decomp.), elem. anal. calc. (%) for $C_{33}H_{45}N_3O_6Ru \times 1.0\ CH_3OH$: C 57.29, H 6.93, N 5.89. Found: C 57.17, H 7.11, N 5.84. ESI MS m/z: 680 $[M - H]^-$, 704 $[M + Na]^+$. ^{1}H NMR (400.13 MHz, $CDCl_3$, δ ppm): 7.85(s, 1H, N-H), 7.79 (s, 2H, C=CH-C), 7.59 (br.s, 1H, N-CH=N), 6.93 (br.s, 1H, N=CH-CH), 6.78 (br.s, 1H, CH=CH-N), 5.54 (s, 1H, O-H), 5.48 (d, 2H, J = 6.0 Hz, C-CH=CH), 5.30 (d, 2H, J = 6.0 Hz, CH=CH-C), 3.81 (t, 2H, J = 7.0 Hz, CH_2-CH_2-N), 3.25-3.21 (m, 2H, NH-CH_2-CH_2), 2.80-2.73 (m, 1H, CH_3-CH-CH_3), 2.11 (s, 3H, C_{Ar}-CH_3), 1.92-1.78 (m, 2H, CH_2-CH_2-CH_2), 1.46 (s, 18H, C-CH_3), 1.26 (d, 6H, J = 6.9 Hz, CH_3-CH-CH_3).

Oxalato(η^6-*p*-cymene){*N*-[3-(1*H*-imidazol-1-yl)propyl]-2-(3,5-di-*tert*-butyl-4-hydroxyphenyl)acetamide}ruthenium(II) (**6**)

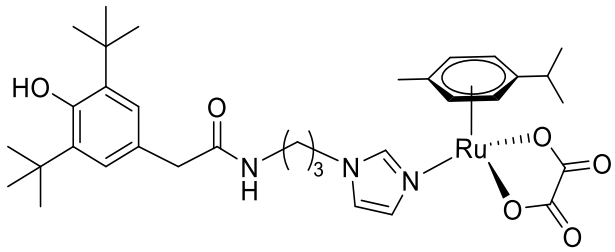

A suspension of silver oxalate (82 mg, 0.28 mmol) in water (10 ml) was added to a solution of bis[dichlorido(η^6-*p*-cymene)ruthenium(II)] (82 mg, 0.14 mmol) in water (27 ml). The reaction mixture was stirred at room temperature for 12 h. The solution was filtered, and the solvent was removed. The solid product was dissolved in MeOH (17 ml) and added to a solution of **2** (100 mg, 0.28 mmol) in a minimum amount of MeOH. The reaction mixture was stirred at room temperature for 12 h. The product was purified by column chromatography on silica gel (eluent: EtOAc : MeOH (2:1), R_f = 0.50). The obtained yellow product was dried in a vacuum. Yield: 137 mg (75%), m.p. 215–220°C (decomp.), elem. anal. calc. (%) for $C_{34}H_{47}N_3O_6Ru \times 0.5\ CH_2Cl_2$: C 56.20, H 6.56, N 5.70. Found: C 56.15, H 7.06, N 6.05. ESI MS m/z: 718 $[M + Na]^+$. ^{1}H NMR (400.13 MHz, $CDCl_3$, δ ppm): 8.1(t, 1H, J = 5.5 Hz, N-H), 7.97 (br.s, 1H, N-CH=N), 7.30 (br.s, 1H, N=CH-CH), 6.99 (s, 2H, C=CH-C), 6.77 (br.s, 1H, CH=CH-N), 6.80 (s, 1H, O-H), 5.70 (d, 2H, J = 6.1 Hz, C-CH=CH), 5.46 (d, 2H, J = 6.1 Hz, CH=CH-C), 4.01 (t, 2H, J = 6.8 Hz, CH_2-CH_2-N), 2.97 (q, 2H, J = 6.3 Hz, NH-CH_2-CH_2), 2.68-2.62 (m, 1H, CH_3-CH-CH_3), 2.50-2.48 (m, 2H, C_{Ar}-CH_2-CO), 2.0 (s, 3H, C_{Ar}-CH_3), 1.88-1.77 (m, 2H, CH_2-CH_2-CH_2), 1.34 (s, 18H, C-CH_3), 1.17 (d, 6H, J = 6.9 Hz, CH_3-CH-CH_3).

Sodium *trans*-terachloro(dimethyl sulfoxide){*N*-[3-(1*H*-imidazol-1-yl)propyl)-3,5-di-*tert*-butyl-4-hydroxybenzamide}ruthenate(III) (**7**)

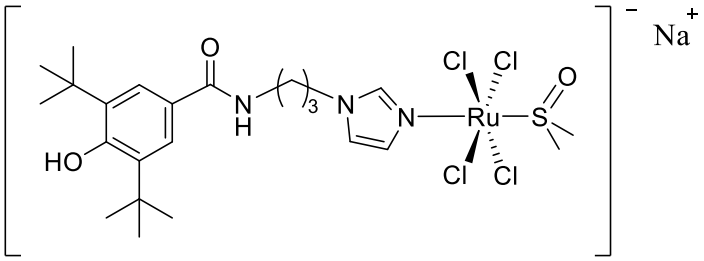

A suspension of **1** (30 mg, 0.08 mmol) in acetone (5 mL) was added to a solution of $[Ru(DMSO)_2Cl_4]^-Na^+$ (35 mg, 0.08 mmol) in acetone (10 mL). The reaction mixture was stirred at room temperature for 12 h. The product was purified by column flash chromatography on silica gel (eluent: acetone : petroleum ether (2:1). The obtained red-brown product was dried in a vacuum. Yield: 45 mg (78%), m.p. 173–176°C (decomp.), elem. anal. calc. (%) for $C_{23}H_{37}Cl_4N_3O_3SRuNa \times 0.5\ C_3H_6O$: C 40.33, H 5.49, N 5.76. Found: C 40.67, H 5.49, N 5.79. ESI MS m/z: 679 $[M - Na]^-$.

Sodium *trans*-tetrachloro(dimethyl sulfoxide){*N*-[3-(1*H*-imidazol-1-yl)propyl]-2-(3,5-di-*tert*-butyl-4-hydroxyphenyl)acetamide}ruthenate(III) (**8**)

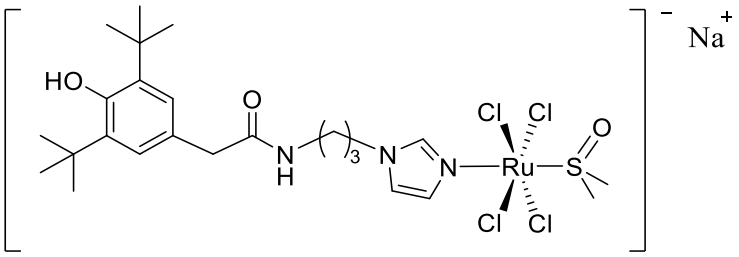

A solution of **2** (50 mg, 0.14 mmol) in acetone (10 mL) was added to a solution of $[Ru(DMSO)_2Cl_4]^-Na^+$ (57 mg, 0.14 mmol) in acetone (20 mL). The reaction mixture was stirred at room temperature for 12 h. The product was purified by column chromatography on silica gel (eluent: acetone : petroleum ether (2:1), $R_f = 0.30$). The obtained red-brown product was dried in a vacuum. Yield: 69 mg (72%), m.p. 124–128°C (decomp.), elem. anal. calc. (%) for $C_{24}H_{39}Cl_4N_3O_3SRuNa$: C 40.29, H 5.49, N 5.87. Found: C 40.29, H 5.73, N 5.65. ESI MS m/z: 693 $[M - Na]^-$.

3.2. CUPRAC assay

The method proposed by Apak *et al*. was used with slight modification.[S3] For these measurements 50 µL of acetate buffer solution at pH 7.0 (1 M), 50 µL of water $CuCl_2$ solution (10 mM), 50 µL of methanol neocuproine solution (7.5 mM) and 50 µL of tested compound (or standard) solution were added to a 96-well plate. All organic ligands and ruthenium complexes solutions were freshly prepared in methanol at 250 µL and 25 µL concentration, respectively, before measurement. The absorbance was measured at 450 nm on a Multiskan Go microplate spectrophotometer (Thermo Scientific, USA) against a reagent blank. The measurements were carried out at 37°C until the reaction was complete. Results were presented in Trolox equivalents (Trolox Equivalent Antioxidant Capacity, TEAC) obtained from the ratio of the absorbance data of the reaction mixtures containing the tested compounds and Trolox.

3.3. DPPH assay

The method proposed by Brand-Williams et al. was used with slight modification.[S4] For these measurements, 100 µL of ethanol DPPH solution (200 µM) and 100 µL of tested compound solution were added to a 96-well plate. 100 µM ethanol DPPH solution was used as the negative

control. The absorbance was measured at 517 nm on a Multiskan Go microplate spectrophotometer (Thermo Scientific, USA) against a reagent blank. The measurements were carried out at 37°C for 50 min. The antioxidant activity was expressed as the percentage of reduced DPPH according to the formula: I (%) = (A0−A1)/A0·100, where A0 is the absorbance of 100 μM ethanol DPPH solution and A1 is the absorbance of the reaction mixture in the presence of the tested compound.

3.4. Electrochemical study

Cyclic voltammetry experiments were performed with an IPC Pro-M potentiostat using a three-electrode cell (MICRO-CELL K0264). The reference electrode was Ag/AgCl (KCl saturated). Platinum wire was used as the counter electrode. Glassy carbon disk and Pt disk with a diameter 2 mm were used as working electrode. The cyclic voltammograms were recorded at a 100 mV s^{-1} scan rate. Measurements were carried out under argon at room temperature.

The compounds were dissolved in MeCN, containing 0.05 M Bu_4NBF_4 as the supporting electrolyte. The concentration of compounds was 0.001 M. The CH_3CN was preliminarily distilled, collecting the fraction with T_{boil} = 81–82°C/760 Torr.

3.5. Study of the effect of compounds on LP in rat brain homogenate

The antioxidant properties of the synthesized conjugates were evaluated by their ability to inhibit lipid peroxidation in the crude membrane fraction (1500 *g*) of the rat brain homogenate.[S5] The brain homogenate in the presence of the test compound or an equal volume of solvent (DMSO) was incubated for 1 hour in the presence of 10 mM H_2O_2 or 0.5 mM $FeNH_4(SO_4)_2$ x 12 H_2O. The degree of LP was assessed by the formation of trimetine complexes of secondary LP products with 2-thiobarbituric acid (TBARs). The data were normalized to control and IC_{50} was calculated with nonlinear regression fit (GraphPad Prism v8.0).

3.6. Cells and MTT assay

The human HCT116 colorectal carcinoma, A549 non-small cell lung carcinoma, MCF7 breast adenocarcinoma, and WI38 non-malignant lung fibroblast cell lines were obtained from the European collection of authenticated cell cultures (ECACC; Salisbury, UK). All cells were grown in a Dulbecco's modified eagle medium (DMEM) (Gibco™, Ire-land) supplemented with 10% fetal bovine serum (Gibco™, Brazil). The cells were cultured in an incubator at 37 °C in a humidified 5% CO_2 atmosphere and were subcultured two times a week. The antiproliferative activity was studied by MTT assays as published previously.[S6]

3.7 Stability

The stability of Ru(III) complexes 7 and 8 was studied by electron absorption spectroscopy in 20 mM phosphate buffer pH 7.4, 100 mM NaCl. The working solution (2 ml, 200 μM com-plex) was prepared by diluting 10 μl of the original 40 mM solution in DMSO and 1.99 ml of phosphate buffer. UV-vis spectra were recorded every 60s in the range 280-600 nm at 37°C. The half-transformation time $t_{1/2}$. For λmax, ΔA(*t*) was plotted, where ΔA = A0-Ai, an initial section was approximated as a linear function. AtΔAline./2 point calculated $t = t_{1/2}$.

Schemes, Figures and Tables

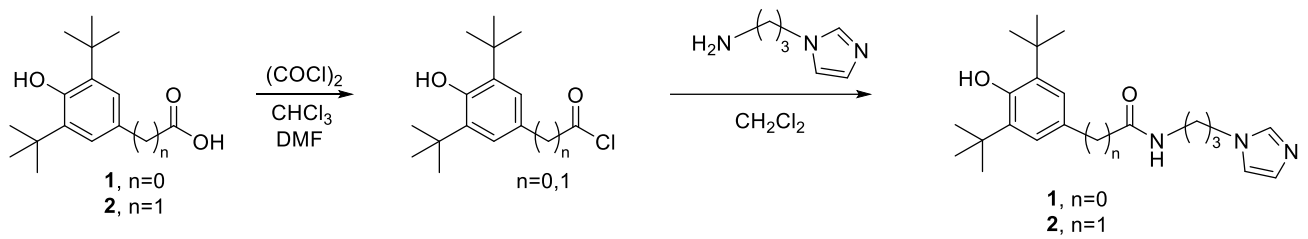

Scheme S1. Synthesis of ligands.

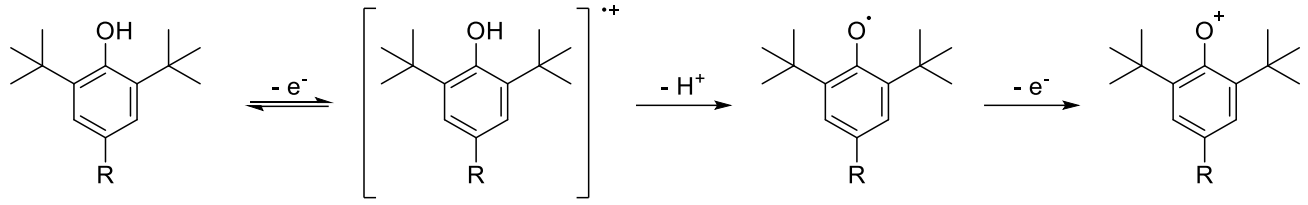

Scheme S2. Mechanism of 2,6-di-*tert*-butylphenol group oxidation: the first electron transfer leads to the cation-radical appearance, following by fast deprotonation and second one-electron oxidation leading to cation formation.

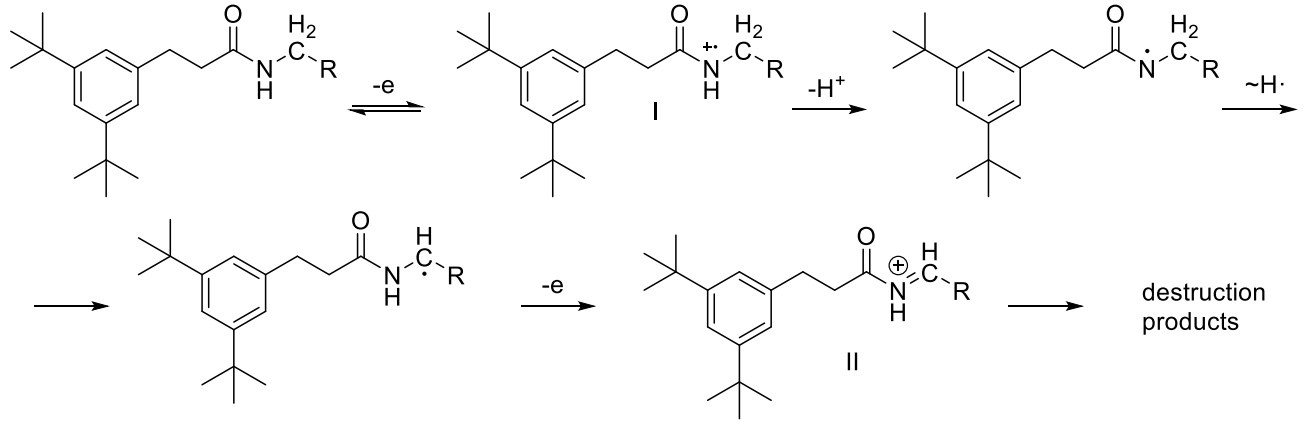

Scheme S3. Feasible mechanism of electrochemical oxidation of compound **1b**: the first peak can be associated with N-centered one-electron oxidation of amide group, resulting in the formation of radical cation **I** and followed by fast deprotonation. The second peak at more anodic potentials corresponds to further one-electron oxidation of methylene fragment that leads to the formation of N-acylium cation **II**.

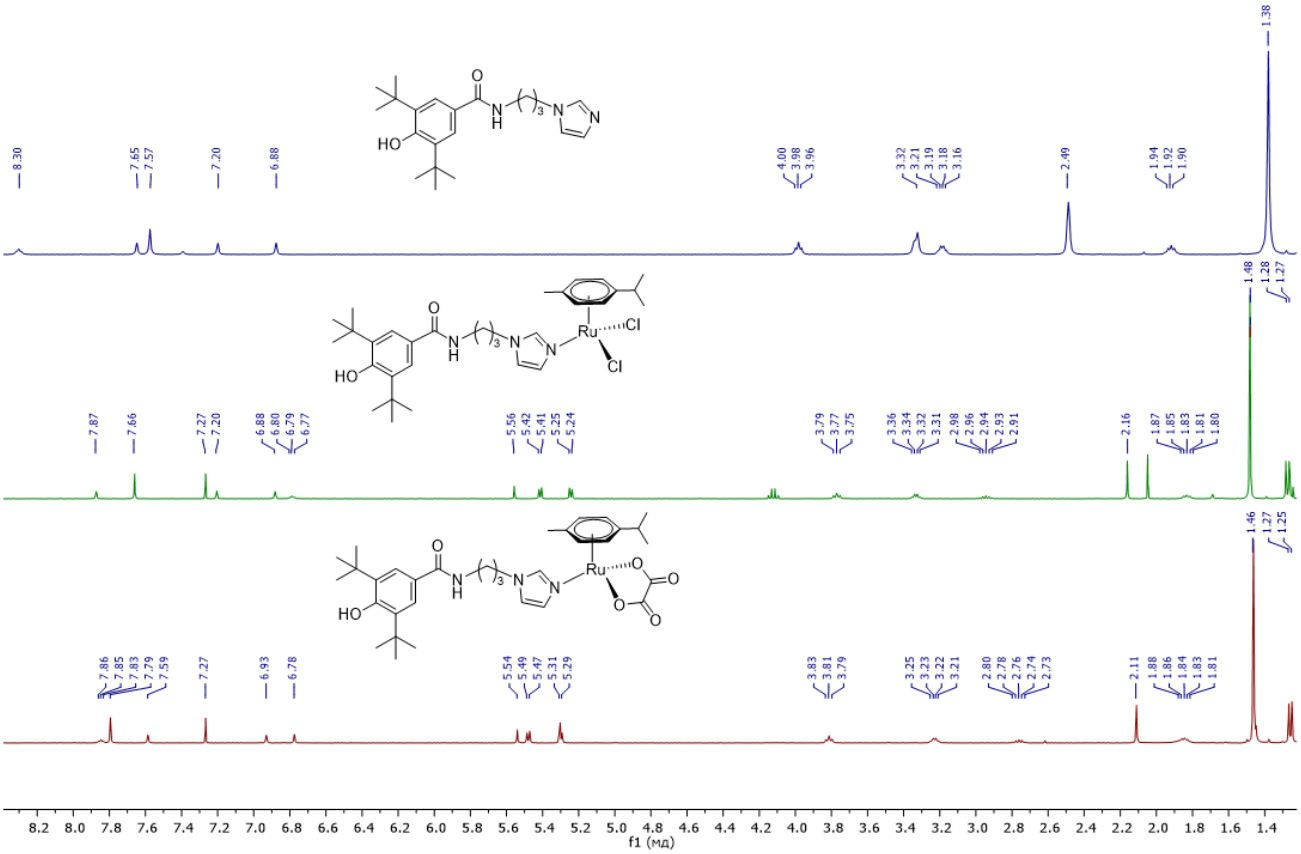

Figure S1. ^{1}H NMR spectra of **1**, **3** and **5** in $CDCl_3$.

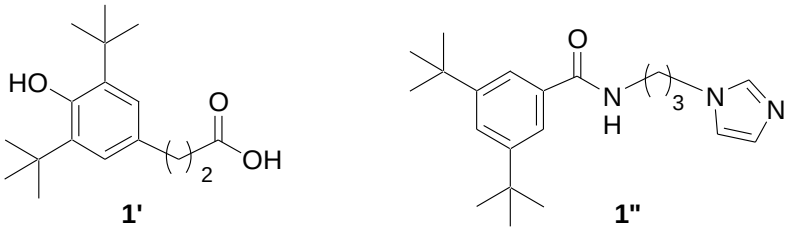

1' **1"**

Figure S2. Structures of compounds **1'** and **1"**.

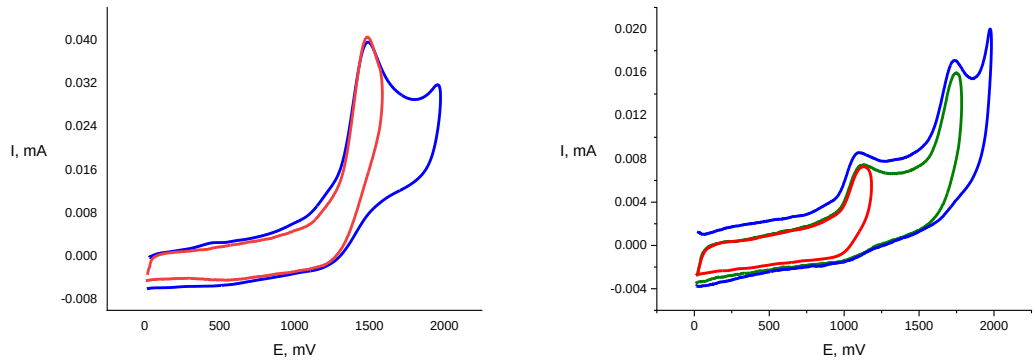

(*a*) (*b*)

Figure S3. The cyclic voltammogram in the anodic range (MeCN, GC electrode, C = 10^{-3} M, $5\cdot10^{-2}$ M Bu_4NBF_4, scan rate 100 мV/s, *vs.* Ag|AgCl|KCl(sat.)) of compounds **1'** (*a*) and **1"** (*b*).

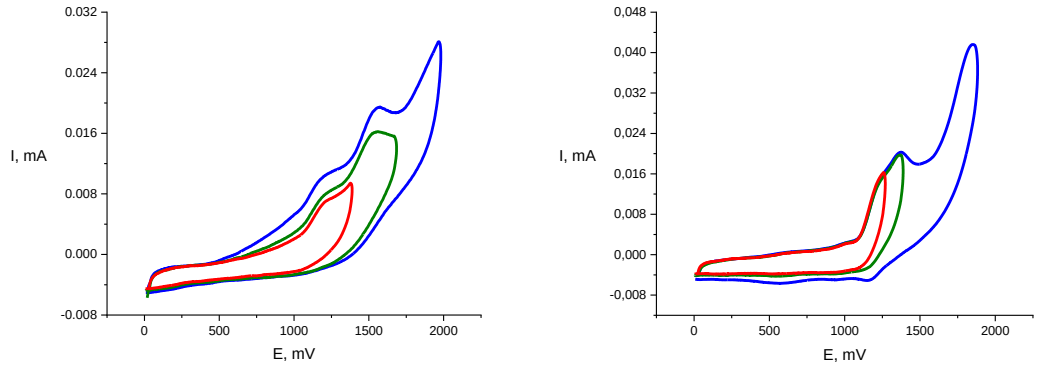

(*a*) (*b*)

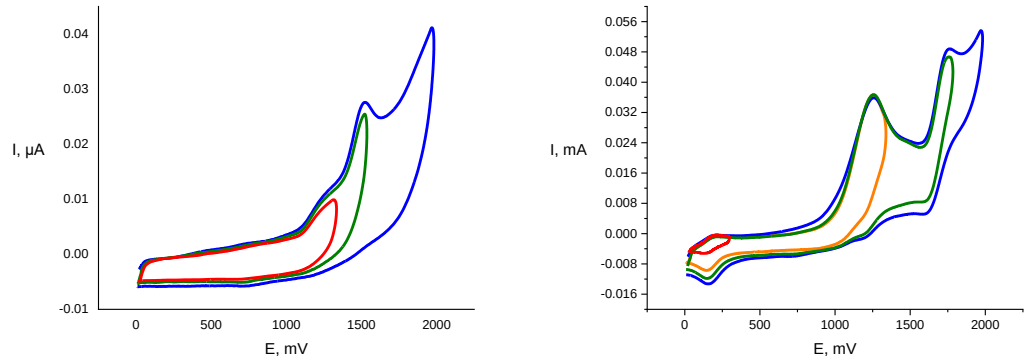

(*c*) (*d*)

Figure S4. The cyclic voltammogram in the anodic range (MeCN, GC electrode, C = 10^{-3} M, $5 \cdot 10^{-2}$ M Bu_4NBF_4, scan rate 100 мV/s, *vs.* Ag|AgCl|KCl(sat.)) of compounds **2** (*a*), **3** (*b*), **5** (*c*) and **8** (*d*).

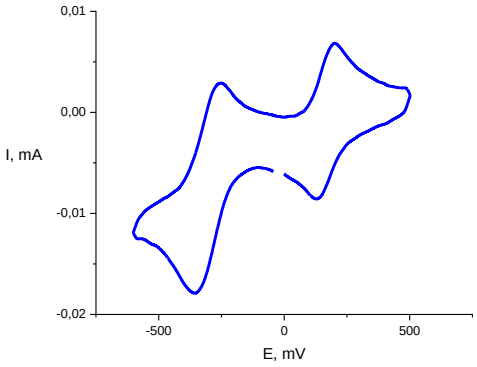

Figure S5. The cyclic voltammogram of compound **8** in the cathodic and anodic range (MeCN, GC electrode, C = 10^{-3} M, $5 \cdot 10^{-2}$ M Bu_4NBF_4, scan rate 100 мV/s, *vs.* Ag|AgCl|KCl(sat.)).

Table S1. Values of oxidation/reduction potentials of **1a, 1b,** ligands **1, 2** and complexes **3–8** (CH_3CN, GC and Pt electrode, C = 10^{-3} M, $5 \cdot 10^{-2}$ M n-Bu_4NBF_4, scan rate 100 мV/s, vs. Ag|AgCl|KCl(sat.)).

Compound	E^{Ox}, V				E^{Red}, V	
	$E^{Ox}{}_1$	$E^{Ox}{}_2$	$E^{Ox}{}_3$	$E^{Ox}{}_4$	$E^{Red}{}_1$	$E^{Red}{}_2$
GC electrode						
1'	1.49	-	-	-	-1.33	-
1"	1.12	1.74	-	-	-0.87	-
1	1.23	-	-	-	-0.95	-
2	1.20	1.55	-	-	-1.11	-
3	1.25	1.37	1.85/1.15*	-	-1.11	-1.45
4	1.31	1.51	1.65	1.85/1.14*	-	-1.48
5	1.23	1.52	-	-	-	-1.58
6	1.29	1.56	-	-	-	-1.54
7	0.23/0.11*	-	1.29	1.83/1.63*	-0.39/-0.24*	-
8	0.25/0.11*	-	1.34/1.20*	1.90/1.62*	-0.36/-0.26*	-
Pt electrode						
1'	1.49	-	-	-	-0.93/-0.64*	-
1"	1.18	1.86	-	-	-1.22/-0.35*	-
1	1.19	-	-	-	-1.55/-1.58*	-0.55
2	-	-	-	-	-1.49/-1.50*	-0.70
3	1.39	1.70	1.87/1.15	-	-1.24	-1.49
4	-	1.54	1.91/1.12	-	-	-1.48
5	-	1.60	-	-	-	-1.42
6	1.32	1.62	-	-	-0.78	-
7	0.21/0.14*	-	1.24	1.74/1.61*	-0.37/-0.25*	-
8	0.21/0.15*	-	1.26/1.20*	1.76/1.61*	-0.37/-0.25*	-

* The peak appears at the reverse scan of potential.

Table S2. MTT assay results (72 h cell exposure).

Compound	IC_{50}, μM			
	A549	WI38	HCT116	MCF7
1	>100	>100	>100	>100
2	>100	>100	80 ± 9	>100
3	69 ± 9	85 ± 18	51 ± 7	50 ± 2
4	88 ± 6	96 ± 1	80 ± 2	54 ± 2
5	77 ± 4	87 ± 16	44 ± 1	63 ± 17
6	>100	>100	42 ± 3	84 ± 14
7	>100	>100	>100	>100
8	>100	>100	>100	>100

NMR and MS spectra of compounds

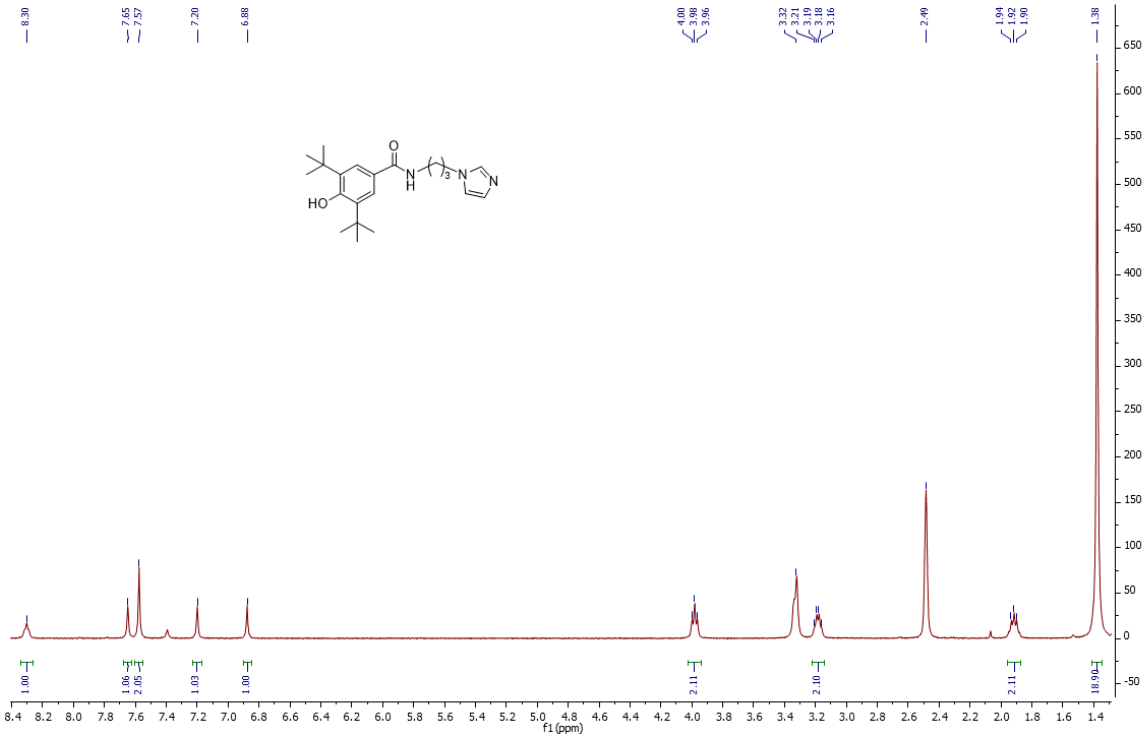

Figure S6. H^1 NMR spectrum of **1** in $CDCl_3$.

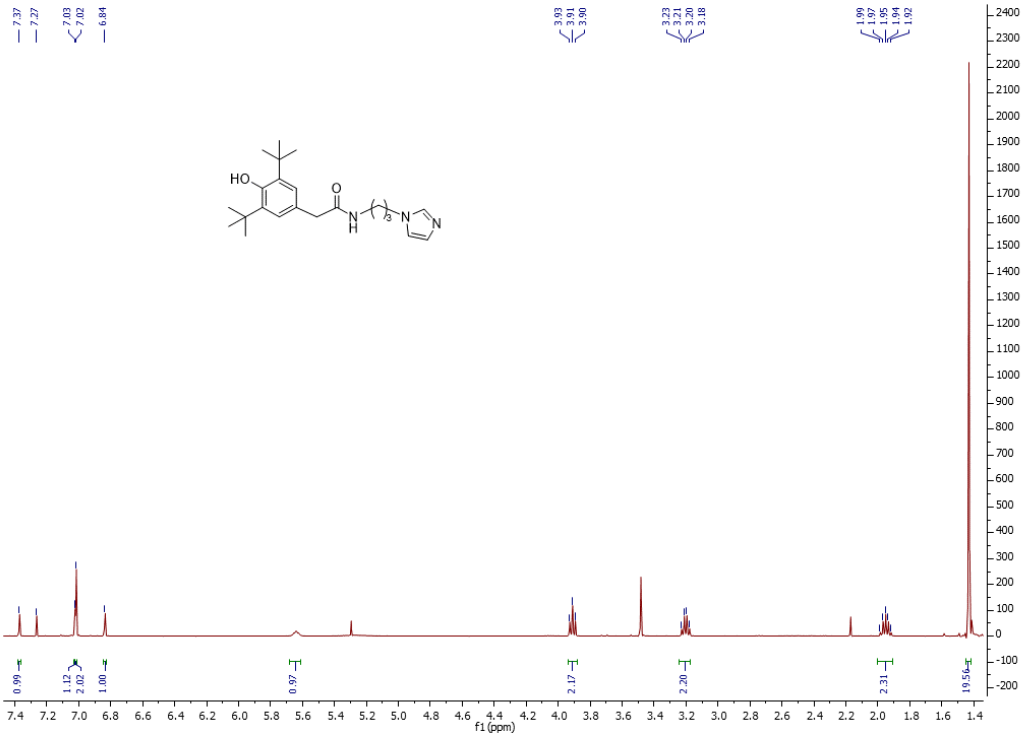

Figure S7. H^1 NMR spectrum of **2** in $CDCl_3$.

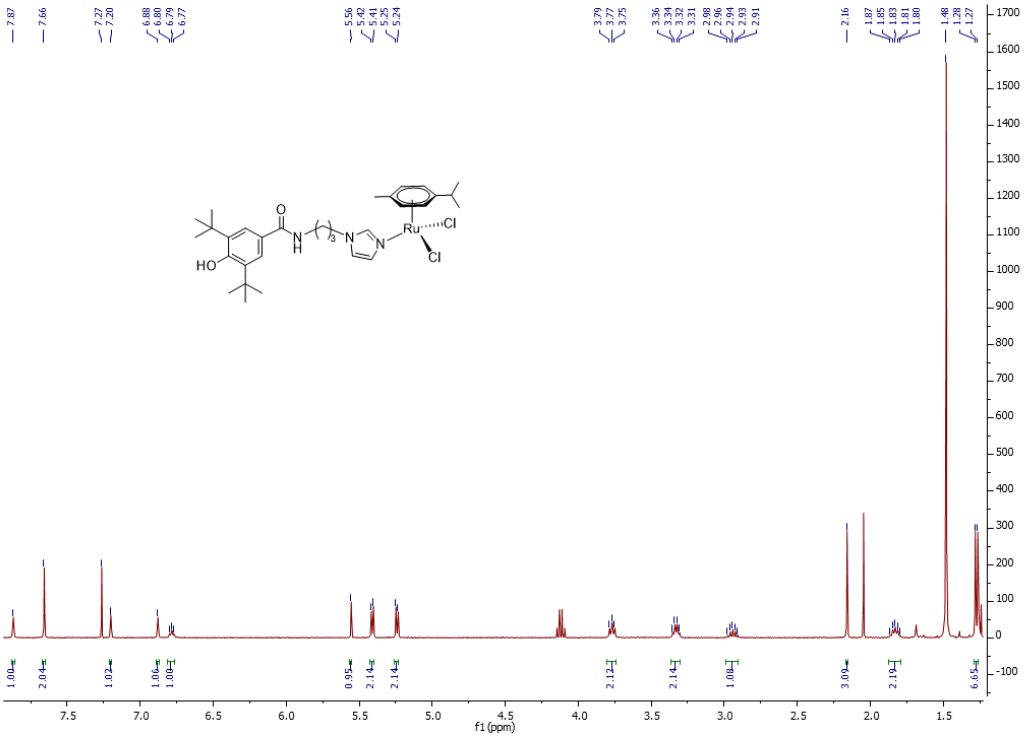

Figure S8. H^1 NMR spectrum of **3** in $CDCl_3$.

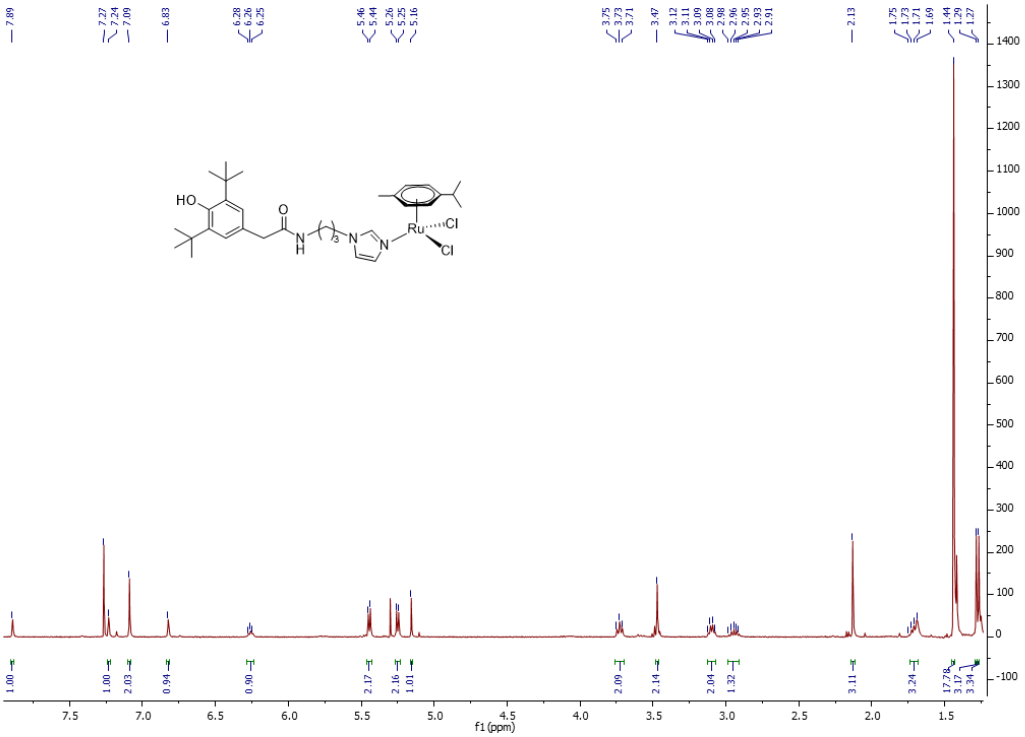

Figure S9. H^1 NMR spectrum of **4** in $CDCl_3$.

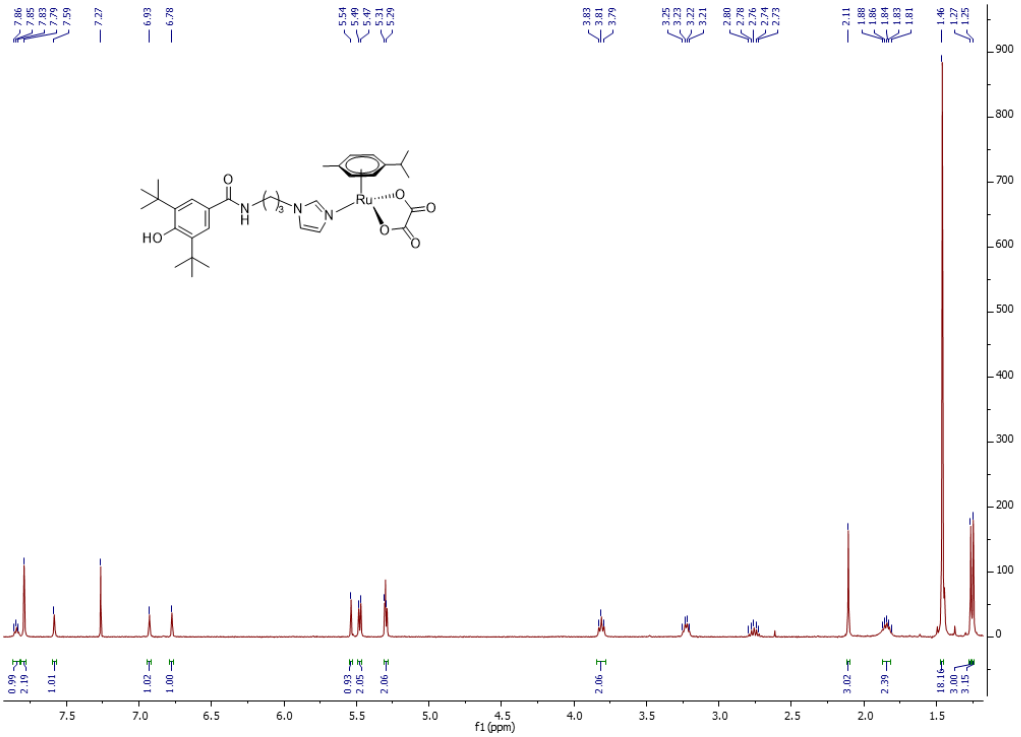

Figure S10. H^1 NMR spectrum of **5** in $CDCl_3$.

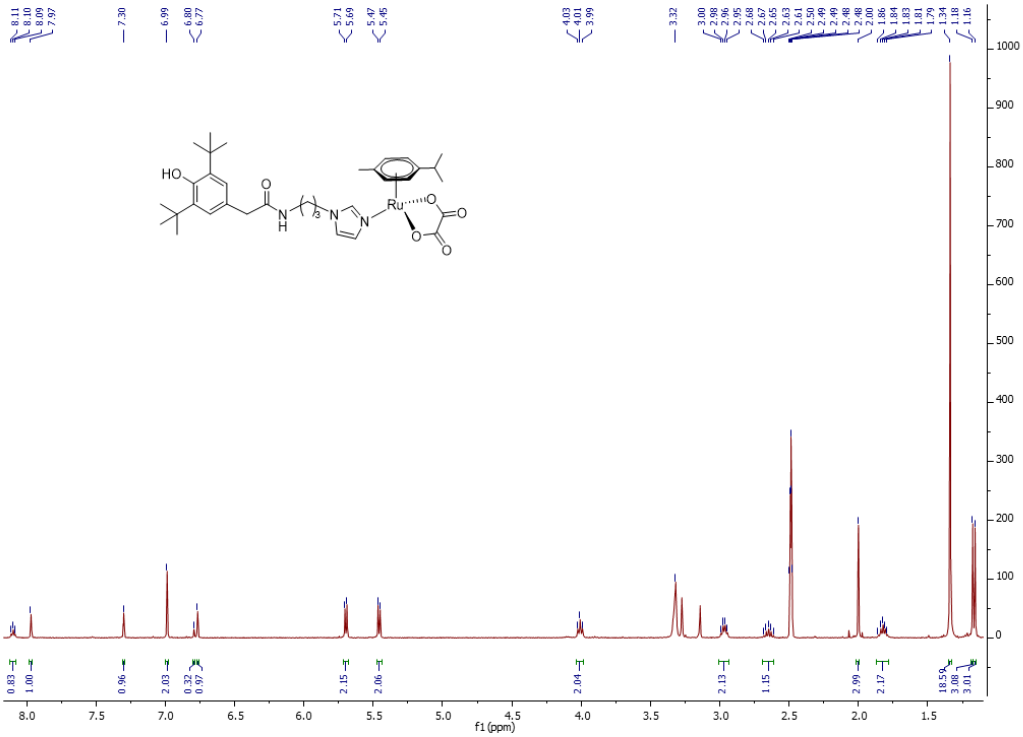

Figure S11. H^1 NMR spectrum of **6** in DMSO.

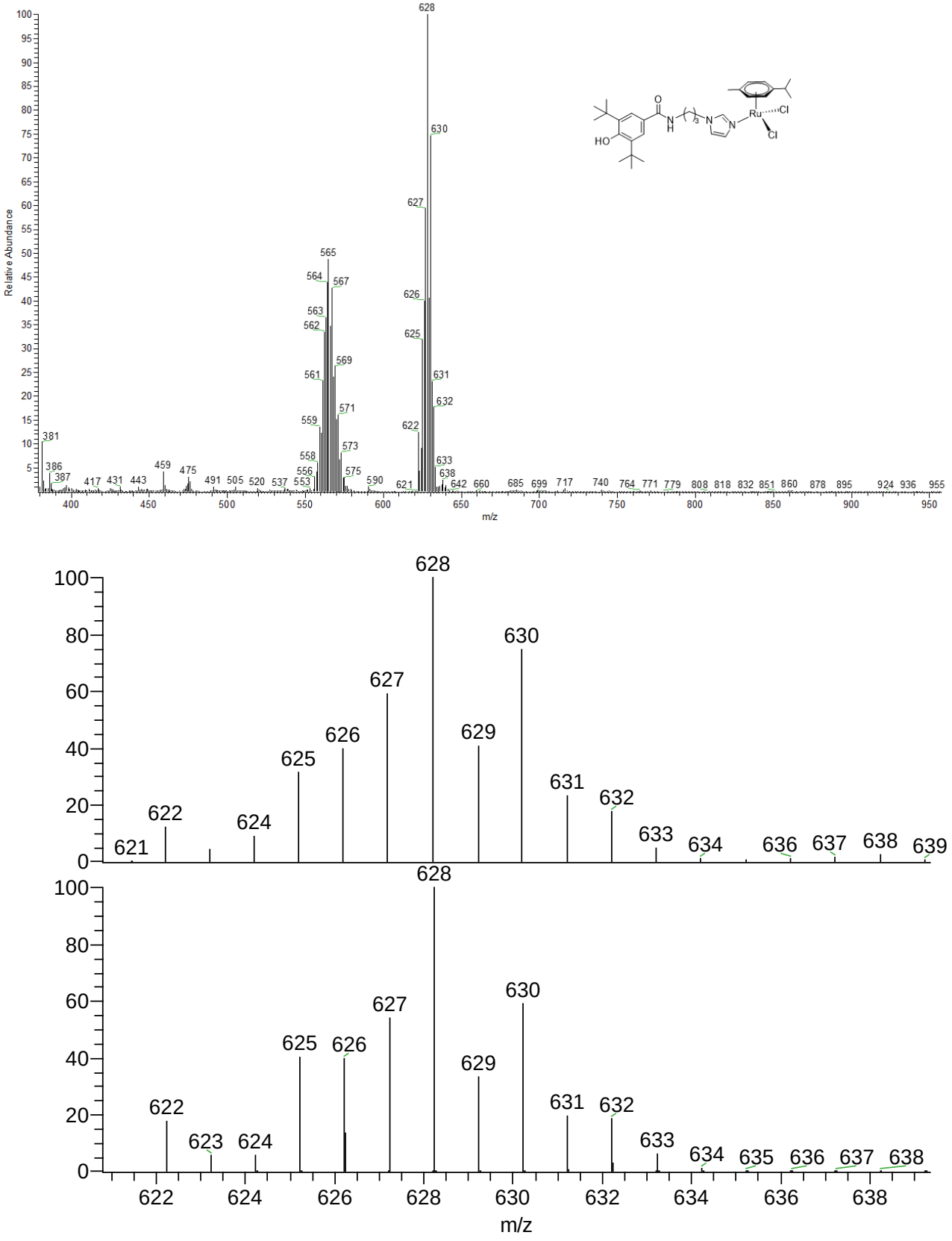

Figure S12. ESI mass spectrum of compound **3** (experimental at the top and in the middle, calculated at the bottom).

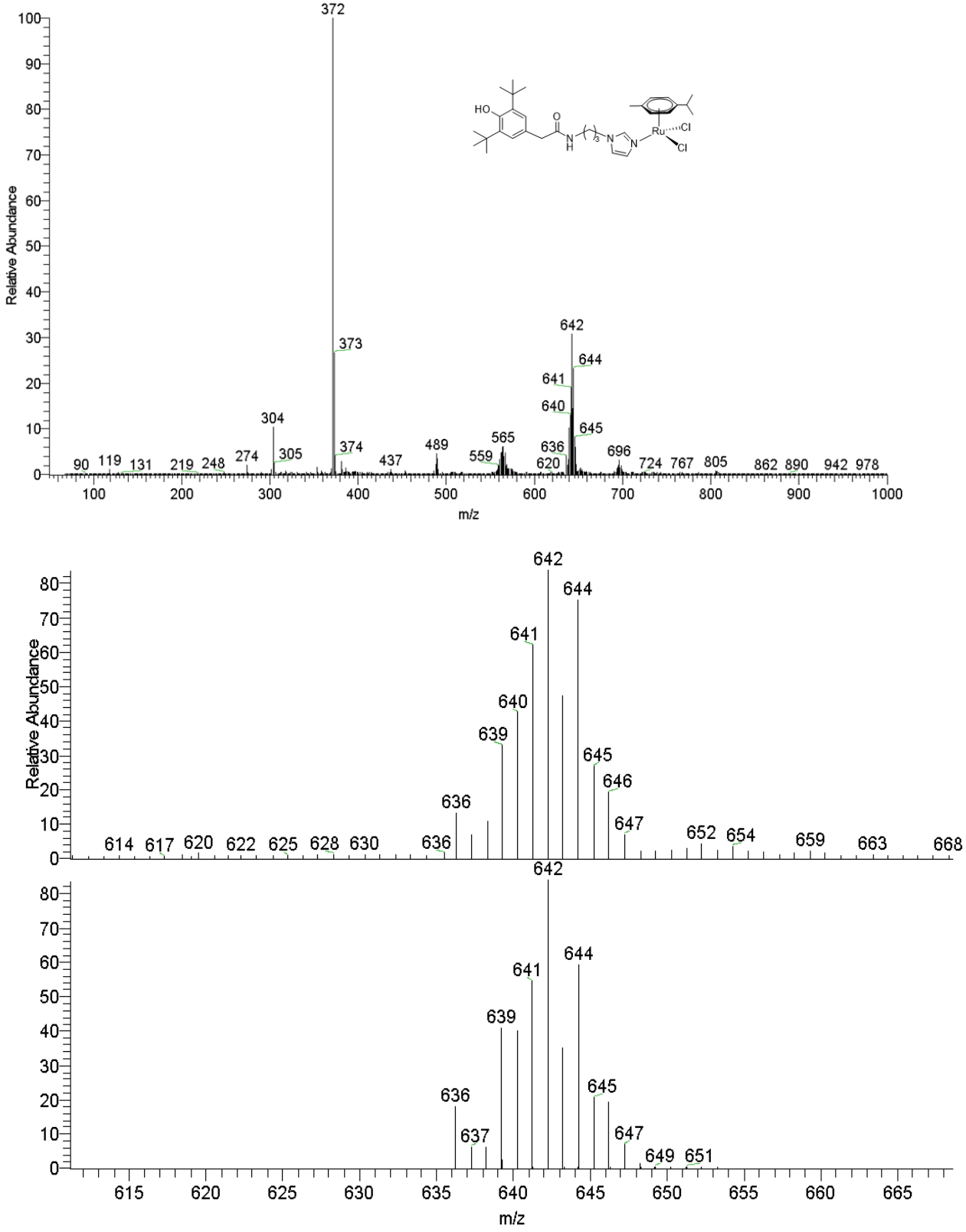

Figure S13. ESI mass spectrum of compound **4** (experimental at the top and in the middle, calculated at the bottom).

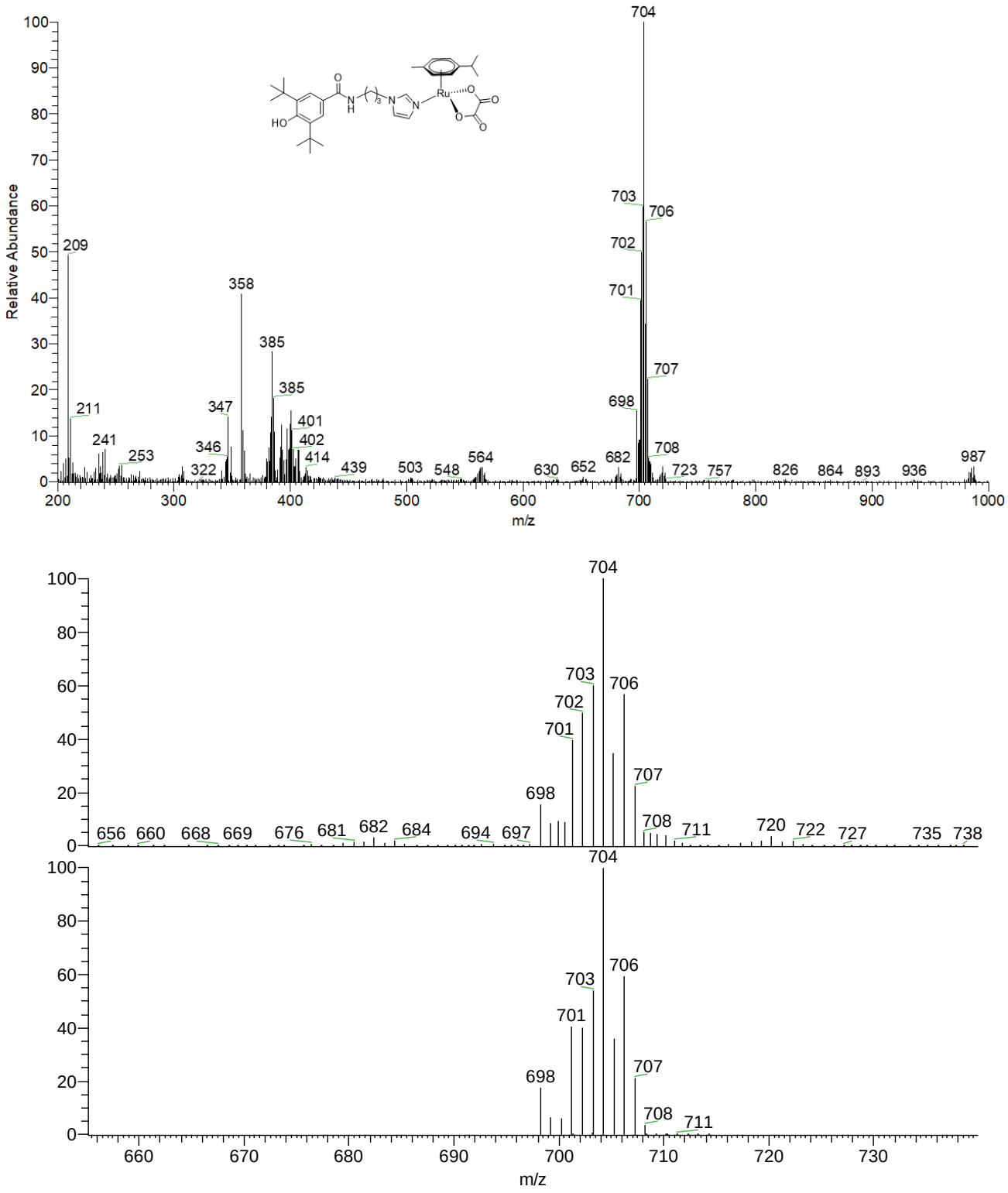

Figure S14. ESI mass spectrum of compound **5** (experimental at the top and in the middle, calculated at the bottom).

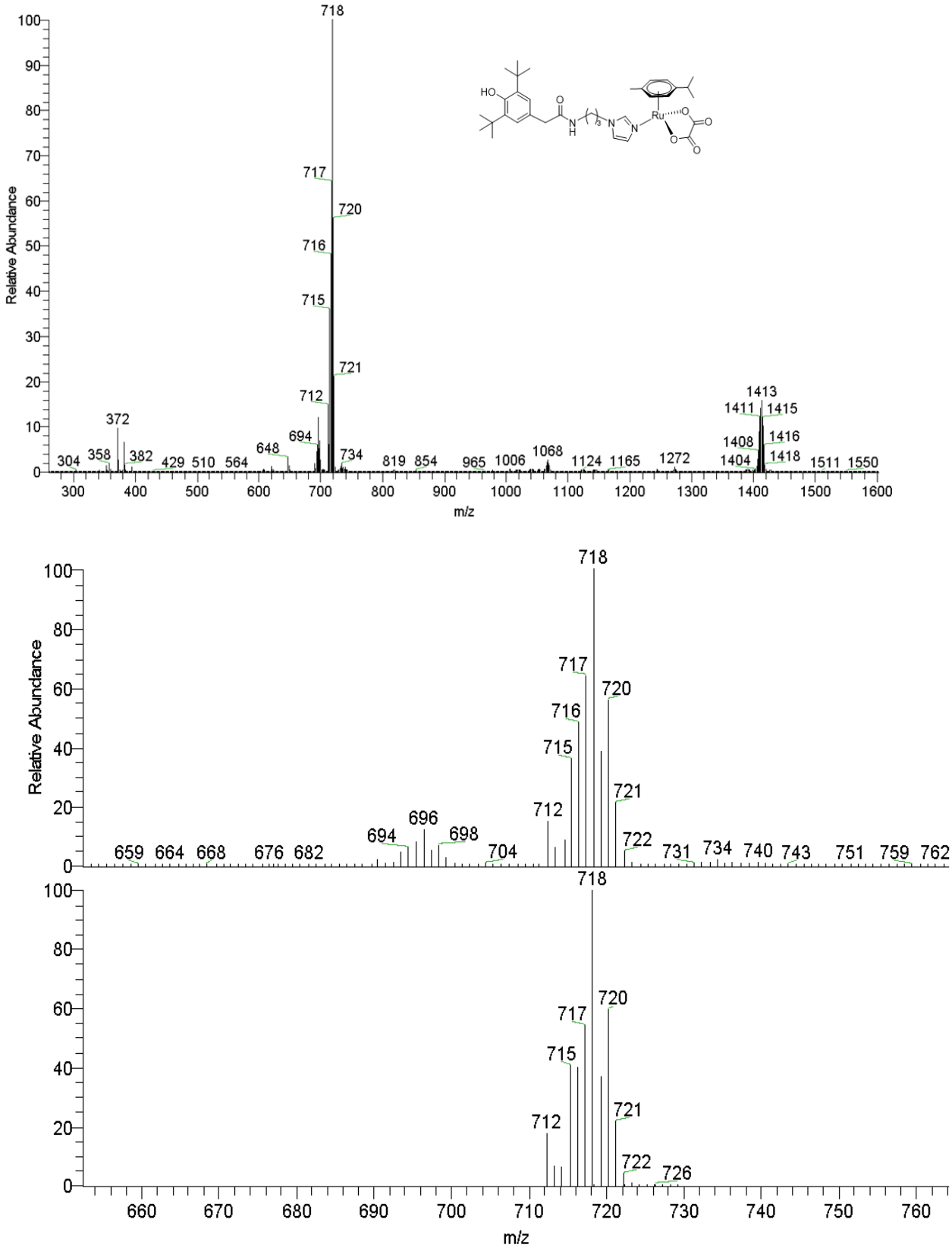

Figure S15. ESI mass spectrum of compound **6** (experimental at the top and in the middle, calculated at the bottom).

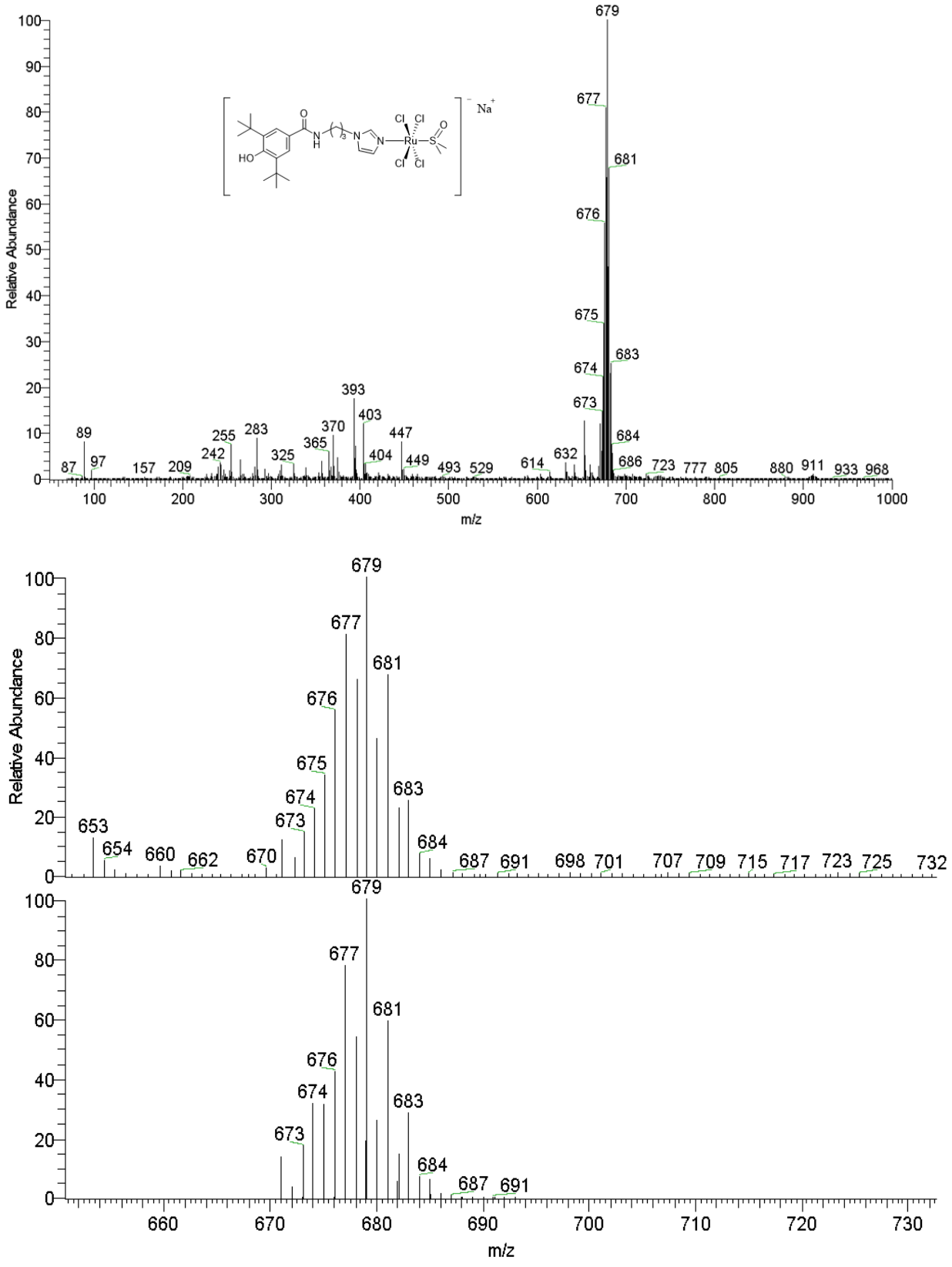

Figure S16. ESI mass spectrum of compound **7** (experimental at the top and in the middle, calculated at the bottom).

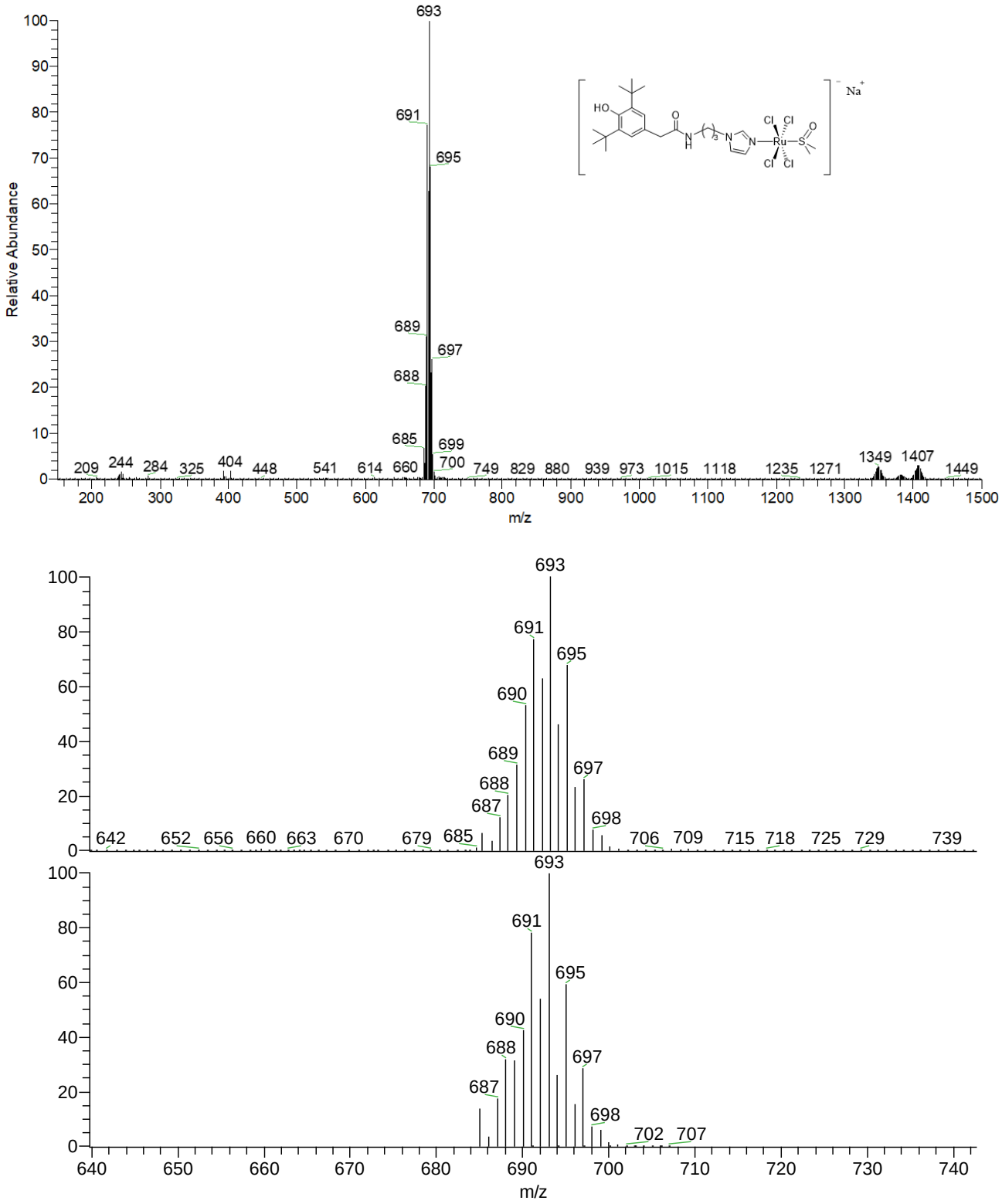

Figure S17. ESI mass spectrum of compound **8** (experimental at the top and in the middle, calculated at the bottom).

References

S1. W. L. F. Armarego and C. L. L. Chai, *Purification of Laboratory Chemicals*, 5th edn., Butterworth-Heinemann, 2003.

S2. E. A. Nikitin, D. B. Shpakovsky, V. Yu. Tyurin, A. A. Kazak, Yu. A. Gracheva, V. A. Vasilichin, M. S. Pavlyukov, E. M. Mironova, V. E. Gontcharenko, K. A. Lyssenko, A. A. Antonets, L. G. Dubova, P. N. Shevtsov, E. F. Shevtsova, M. A. Shamraeva, A. A. Shtil and E. R. Milaeva, *J. Organomet. Chem.*, 2022, **959**, 122212.

S3. R. Apak, K. Güçlü, M. Özyürek and S. E. Karademir, *J. Agric. Food. Chem.*, 2004, **52**, 7970.

S4. W. Brand-Williams, M. E. Cuvelier and C. Berset, *LWT - Food Sci. Technol.*, 1995, **28**, 25.

S5. G. F. Makhaeva, E. Shevtsova, N. P. Boltneva, N. V. Kovaleva, E. V. Rudakova, L. G. Dubova, P. N. Shevtsov and S. Bachurin, *Dokl. Biochem. Biophys.*, 2019, **484**, 1.

S6. Y. N. Nosova, L. S. Foteeva, I. V. Zenin, T. I. Fetisov, K. I. Kirsanov, M. G. Yakubovskaya, T. A. Antonenko, V. A. Tafeenko, L. A. Aslanov, A. A. Lobas, M. V. Gorshkov, M. Galanski, B. K. Keppler, A. R. Timerbaev, E. R. Milaeva and A. A. Nazarov, *Eur. J. Inorg. Chem.*, 2017, 1775.